Computing and Informatics, Vol. 45, 2026, 439–457, doi: 10.31577/cai_2026_2_439

DEEP LEARNING AND SINGLE PHOTON EMISSION COMPUTED TOMOGRAPHY WITH MULTI-CLASS SEGMENTATION MAPS FOR BRAIN TUMOR CLASSIFICATIONS

J. Hima Bindu, M. Uma Devi

Department of Computer Science and Engineering
Vignan's Foundation for Science, Technology and Research
(Deemed to be University)
Vadlamudi, Guntur – 522213, Andhra Pradesh, India
e-mail: Jhimabindu_it@mgit.ac.in, druma_cse@vignan.ac.in

Abstract. Computerized segmentation and classification of brain tumors are essential for diagnosis, management, and prediction of the prognosis in neuro-oncology. Standard methodologies for the diagnosis of brain tumors are subjective, based on human experience and qualitative analysis of images, which makes them unsuitable for handling all the variability in tumor types. To address these challenges, this research presents an innovative approach of combining DCNs and PECT images to accurately and quickly segment and classify multi-class brain tumor. The framework uses a DenseNet architecture tailored for high-resolution functional imaging in PECT to yield rich feature representations for tumor identification as well as grading and staging for several types of tumors. The computer algorithm was trained on PECT scans of 250 patients with gliomas, meningiomas and metastatic brain tumors as a training set and test set. Proper segmentation of tumor boundaries, type of tumor, and other important structures were carried out using the multi-class segmentation maps. By implication, the experimental results show that the proposed model has a classification accuracy of 94 %, which was higher than PECT-based approaches by 2 %. The generated segmentation maps also yield essential sparsely rendered images which really help the surgeon understand the tumour's size, position and relationship to adjacent structures and provide better planning and strategy in the treatment process. The framework was able to handle problems arising from the heterogeneity of tumor appearances and the spatial distribution in complicated neuro-oncology cases. This work underscores the role of the latest deep learning approaches in enhancing diagnostic accuracy and the ability to concurrently combine new imaging systems. In future studies, further work will be directed to the increased robustness achieved with the utilization of further imaging, enlarging the dataset for different demographics, and the testing of the proposed framework on more clinical scenarios.

Keywords: Dense convolutional network, photon emission computed tomography, brain tumor classification, multi-class segmentation, deep learning, neuro-oncology, medical imaging

Mathematics Subject Classification 2010: 68T05, 68U10

1 INTRODUCTION

The skill in finding or diagnosing various diseases has become increasingly involved in digital medical imaging. In addition to diagnostics, EMI has a great deal of utilizations in research and medical education, where it provides extraordinarily accurate data as to the various physiological and pathological mechanisms that are occurring within the human body. This reliance on imaging technologies, for example, was captured by the assessment of the modern scale of operation of radiology departments [1]. For example, in 2002, the Radiology Department of the University Hospital of Geneva produced between 12 000 and 15 000 images in a single day, demonstrating the huge amount of data that needed proper and fast assessment [2]. To work with such data, certain and accurate tools are mandatory to provide proper CAD systems to create effective and accurate medical reports or to conduct numerous studies. Categorization of medical images using conventional standard methods was still a slow and error-prone process, and underlines the necessity of more advanced diagnostic systems. Cancers, a global health risk, occupy 10 % of sickness afflictions in the United States and constitute one of the highest death rates [3]. The American Cancer Society reported that over 700 000 people in the United States are diagnosed with benign brain tumors today, of which only 20 % are malignant. The estimation of diagnosis of the primary brain tumor in 2021 by the American Cancer Society was 78 980, out of which 24 530 was malignant (13 840 males and 10 690 females) and 55 150 was non-cancerous. The above statistics demonstrate the increasing prevalence of brain tumors among both children and adults, and their function as the primary cause of cancer-related mortality globally [4]. Tumor of the brain or neuronal cell growth that are uncontrollable are termed brain tumors, and can either be primary or secondary. The majority of primary brain tumors develop from cells within the brain, while secondary or metastatic brain tumors originate from other parts of the body. Both primary and metastatic brain tumors can be further categorized as benign or malignant. Though benign neoplasms do not infiltrate adjacent structures, are slow growing and rarely produce symptoms, they differ from malignant neoplasms significantly. The WHO has a system of grouping brain tumors based on grade: Grade I to

Grade IV. Grade I tumors are most often benign and the tumor was slowly proliferating; in appropriate treatment, the overall prognosis was favourable [5]. Grade II tumors are malignant but grow more slowly than those in a Grade III. Nevertheless, Grade III tumors, which are also known as anaplastic and Grade IV tumors such as glioblastomas, are considered the most invasive types of brain cancer [6]. These are high-grade tumors characterised by a high rate of proliferation, locally invasive nature and intrinsic refractoriness to conventional treatments, which gives them a poor prognosis [7]. Since the treatment of brain tumors was still challenging and many were fatal, early and precise diagnosis was important [8]. Incorporation of new techniques in imaging and diagnostic systems provides improved solutions to the challenges with the opportunities of defining the perimeters of a tumor, distinguishing the types of a tumor and even creating plans for the treatment of the tumor [9]. The convergence of the novel computational tools, using deep learning algorithms, with imaging sciences in the field of diagnostics of brain tumors was expected to deliver increased speed and precision in clinical practice [10]. Grade I and II tumors are the slow-growing and less intrusive in comparison to the Grade III and IV. Initial grades (Grade I) tumors are normally non-cancerous and therefore are often treatable. At this level tumors are malignant, but grow at a slow rate compared to higher grade tumors. Monitoring and relatively less aggressive treatment at initial stages, but can emerge over time [11, 12]. In the last few years, several new imaging technologies have been developed, including ultrasonography, magnetic resonance imaging, computed tomography, magnetoencephalography, positron emission tomography and electroencephalography [13]. These technical developments promote more accurate diagnosis and treatment methods due to the best knowledge about brain tumors. Because it reduces the patients' exposure to ionising radiation, MRI was previously only applicable for the identification of brain tumors [14, 15]. MRI can be used to define the size, position and shape of the tumor with fairly good accuracy. This unfortunate process of diagnosing the brain cancers was, in most part, associated with the competence of radiologists [16]. Traditionally, with more patients, more data involved, current methods are getting costly and less accurate [17]. The difficulties are linked to sharp differences in size, shape, and level of severity of the same type of brain tumor, as well as similar symptoms of different types of diseases. A patient's prognosis was very poor, and other complications increased from an unclear diagnosis of a brain tumor. Toward the end of the 1990s, there was an increasing desire to produce automatic image processing schemes that would eliminate limitations of diagnostic representations and linked approaches [18]. In the recent past, a number of CAD systems have been proposed to enhance the automatic diagnosis of brain tumor.

The current research landscape in deep learning for brain tumor classification utilizing SPECT predominantly emphasizes foundational segmentation and classification techniques. A notable gap exists in leveraging advanced multi-class segmentation maps capable of addressing the complexity and variability of tumor types in SPECT imaging. Existing approaches often neglect the synergistic potential of integrating multi-modal imaging with deep learning frameworks, which could enhance both diagnostic accuracy and model robustness.

2 RESEARCH METHODOLOGY

The overall process of the proposed DCN-PECT framework is shown in Figure 1. The proposed framework comprises six sequential stages: Preprocessing, Multi-Class Segmentation, Network Architecture Design, Loss Function Optimization, Training, and Model Evaluation. First, the input PECT/SPECT images are preprocessed to improve clarity and remove artifacts. After this, the processed images are put into a multi-class segmentation phase to clearly distinguish between Tumor Core (TC), Enhancing Tumor Regions (ETR), and Normal Tissues (NT). Once the segmented images are produced, they are fed into an Encoder-Bottleneck-Decoder (E-B-D) architecture to extract features and classify tumors. While training, Categorical Cross-Entropy (CCE) loss functions were used as weights to optimize performance. The model's performance is measured by validating it on a separate validation dataset and assessing its ability to segment and classify accurately.

2.1 Pre-Processing

In order to analyse an MRI image, it goes through several highly complex steps in order to get into a shape for analysis. The first stage was centred on excluding obstructions that interfere with the clarity of the image [19]. The elements of an image, generally brought into the system during the imaging phase, are capable of causing disruptions along the rest of the image processing and analysis procedures. After such artefacts have been stripped off, the images are enhanced even further through a process called denoising. Reduction of noise enables to distinguish special features of MRI and creates the grounds for more precise approaches to diagnosing and treating diseases in medicine.

In the early stages of applying MRI preprocessing, the image was converted to grayscale. MRI scans are sometimes in RGB format which are sets of data from three different colors namely the red, green and blue [20]. These channels bring in extra information which was not usually needed when using image scans in diagnosis of certain diseases for their patients. Redundant information go and decreased the amount of data by converting the image to grayscale during the experiment. There are two types of images namely Grayscale images, which remove all other color information to keep only the intensity values retainable and usable in storage; usable and useful in the retention of the structural details of the human brain necessary for analysis [21].

After going through grayscale conversion, filters are used to reduce different sorts of noise that is still present in the image. Gaussian, salt-and-pepper, and speckle noises interfere with the image and its analysis because they conceal important

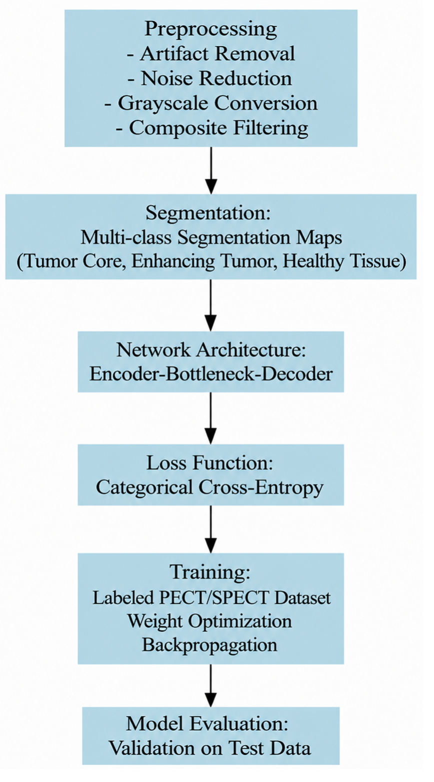

Figure 1. Deep learning and single photon emission computed tomography with multi-class segmentation maps for brain tumor classification

information [22]. To reduce the side effect which was discussed below, a hybrid filter of Gaussian, mean, and median filters were used. All of these filters act on specific kind of noise and the combined application of these filters guarantees a greater extent of noise removal without impacting the edge and boundary characteristics of the image [23].

The main contribution of the composite filter was to work in tandem to ensure that as much noise as possible was filtered out whilst, on the other hand, as many details as possible were preserved. As opposed to the basic filter types that remove image particulars at the expense of important image features, the present technique achieves efficient noise reduction, preserving the MRI image's anatomical features. This additional step enhances the quality of images before being subjected to image segmentation and classification processes, which would help bring about enhanced diagnosis.

2.2 Segmentation

Another important phase in the context of medical imaging was multi-class segmentation which was significant for discriminating the classification of each pixel in an image over different groups, especially in the case of investigations on brain tumors [24]. This classification allows a better insight into the structure of the tumor through the division into the necrotic core of the tumor, the ring on the T1-weighted images where tumor cells are actively enhancing, and the surrounding brain tissue. This pixel-level categorization was crucial for generating accurate representations of the tumor that enable a clinical diagnosis, treatment plan, and follow-up on the progression of the disease [25]. The dividing of tumors into sectors helps medical practitioners determine which regions need to be treated and which do not.

Segmentation was based on complex computations of spatial and structural properties of medical images [26]. State-of-the-art deep learning architectures including U-net is often used for multi-class segmentation because of the high accuracy and applicability to varied datasets. These models use of convolutional and deconvolutional layers, encode spatial information from the input and then decode it to segmentation maps [27]. All layers of the network help to identify certain features, which allows effectively dividing the image into classes. These benefits make this imaging technique ideal for the detection of smaller variations, as in this case, the edges or boundary of the tumor were easily discerned [28].

The quality and resolution of input data also affected the outcome of segmentation, together with the training strategy of the deep learning models. MRI and PECT are generally used because other techniques, such as CT scan or superior resolution and delineation of structures in the brain compared to other imaging instruments, for example. The features include noise reduction based on median filtering and conversion of the image into grayscale, since pre-processing was important to ensure getting improved images for segmentation [29]. When building a model, we use loss functions such as cross entropy to guarantee that during training, possible mistakes are minimized and class labels of each pixel are best assigned for producing good segmentation maps.

In clinical practices, most models grounded on multi-class segmentation form a basis for prescription and operations [30]. Therapists can make sound judgments about therapy or surgical margins when specific boundaries of the tumor and various types of tumor areas are defined. Segmented images provide a way of keeping track of the evolution and treatment outcomes of a tumor. The combination of segmentation maps with other diagnostic tools improves disease progression monitoring and individualised patient care. This makes multi-class segmentation an essential tool for enhancing the precision medicine of neuro-oncology.

2.3 Problem Definition

The classification of MRI brain scans into different classes corresponding to different tissues or tumors was a critical data segmentation in the medical imaging and diagnosis. This was true especially in neuro-oncology in which better definition of tumor margins determines therapy and survival [31]. As with the pixels in a CT scan, each pixel in the MRI image has to be assigned to one of the predetermined labels, which includes a healthy tissue, or a tumor core, or enhancing tumor. This classification requires the identification of the detailed structure of the tissue type or pathologic area in the entire brain and, therefore, it requires a pixel-based system [32].

In the case of the model, the segmentation procedure starts with the input MRI image, referred to as I. The role of the segmentation task was to determine a set of K classes, C_1, C_2, ..., C_K that defines the tissue type or regions of the tumor. The model shall also involve a class label $C(i, j)$ for every pixel (i, j) of the image. This approach allows for the distinction between different layers and zones in tissues and defining the pathophysiologically altered regions, which was paramount for evaluating the shape of the tumor and its contact with the adjacent healthy tissue [5].

The segmentation challenge was in its essence a classification problem at the pixel level, and in order to secure high accuracy and dependability, the application of sophisticated mathematical algorithms was inevitable [33]. CNN and other deep learning techniques have risen as the preferred solutions for this problem [34]. These models can detect fine shapes and grainy distortions of pixel densities leading to easier segmentation of complex and diverse areas [35]. These capabilities also make the models label the inputs while maintaining the tiny anatomical and pathological details that doctors need to see.

It helps in cancer staging and treatment planning with the help of a clinician to decide size of the tumor, position of the tumor, and involvement of nearby structures. It contributes to the formulation of individual treatment plans because it makes detailed images of the tumor regions. These insights therefore enhance surgical efficacy, therapeutic techniques, and patient prognoses making it a central cornerstone of current-day imaging and neurology.

2.4 Network Architecture

The network architecture follows a well-established deep learning approach, structured into three key parts: the encoder, the bottleneck and the decoder. Encoder or contracting path takes the responsibility of extracting features from the input image, which can be highly beneficial for the model [36]. It applies convolutional layers cuff with the max-pooling layers to gradually degrade the spatial size while enhancing the depth of the feature map. This process proves beneficial in capturing of higher level views about the richer input. The encoder in a sense just reduces the information to the bare relevant features required for the task at hand [37].

The second component to proceed the encoder was the bottleneck that encapsulates the abstract level of features that the model captures. It functions here as the interface between the encoder and decoder therefore facilitating the accumulation of information in one array before decoding it and expanding it out to the original spatial dimensions. The bottleneck was designed to preserve the salient information obtained by the encoder and forward such information to the decoder [38]. This design proves useful in reducing the image complexity while retaining characteristics appropriate for the subsequent processes [39].

Decoder, or expansive path, was devoted to reconstructing the spatial resolution of an image. This was realized by employing up-convolutions that assist in slowly reconstructing the spatial dimensions. At each of the up sampled features, the decoder also concatenates information from the encoder, thus ensuring that the encoder information was useful for reconstructing the detailed spatial information from earlier layers. These up-convolutions along with concatenations give the network the ability to refine features in the image across the layers till the final layer was reached.

The last layer of the calculated network aimed at providing the map of the class labels for each pixel of the image. Such pixel-level classification allows the network to do more fine-grained segmentation tasks, like finding several regions in retinal images or any other complicated image. These predictions are made by the network through the encoder-decoder structure in use to output a map of the features learned to represent the class probability distribution across the image.

2.5 Loss Function

The categorical cross-entropy was one of the most commonly employed functions in machine learning in classification problems. It calculates the distance between the true class for a given instance and the probability of the class for that instance. Whenever a model gives a prediction, what was returned was the probability distribution of the different classes. This loss function worked to identify by how much the calculated probability distribution deviated from the real distribution so that, under training, this gap could be reduced. Cross-entropy loss measures how well the model was predicting examples and has a property that the smaller the value of the cross-entropy loss, then the better the model's predictions are to the labels.

In the context of brain tumor classification each pixel in the image was labeled in to one of the few classes like core tumor, enhancing tumor or edema. The loss function will now have an idea of the error between the ground truth class of that pixel and the predicted probability distribution of the pixel. Often when the predicted class of a given pixel was nearly the actual class of the pixel the loss value was smaller. On the other hand, if the prediction was wrong the loss increases, that informs the model that the given prediction was not correct.

Categorical cross entropy works by especially comparing the output probability distribution with the actual class labels which are usually in form of one-hot encoded. A 1 was applied to the correct class for each pixel and a 0 for all other classes. The output of the model was a probability vector, and depending on which loss function was used the loss function was to take the difference between the cred prob and the actual labels in log space. This was details through the use of logarithm so that any form of incorrect prediction will be penalized further if the confidence level was high.

This loss function was important specifically for turning deep learning models, including for tasks such as segmentation and classification. In the process of training the model modifies its parameters in order to minimize the categorical cross-entropy loss and its performance for the classification of the correct class for each pixel improves. This makes the model more discriminative in accurately recognizing the tumor regions and healthy tissue, thus could perform better in medical image segmentation.

2.6 Training

The training process by the training network was accomplished with a set of labeled MRI consisting of images of body organs. These features consist of different MRI images and each MRI or every image shown here contains a label that belongs to particular class or in simple words the category of tumor present in that image was defined. These images themselves form the basis of training the model to differentiate between various forms of brain tumors which include gliomas, meningiomas and pituitary tumors. The labeled data used will enable the network to draw correlation between the features of the scans and the associated tumor types.

When the network starts its training process data parameters or weights are initiated and tweaked to reduce the difference between the anticipated output and actual labels. This was called weight optimization, it was a key step in how to increase the accuracy of the model. Through repetitive transformations of the nets weights, the network was trained to recognize patterns of the image that correspond to defined features of tumors. In time the model gets better at recognizing such patterns and it can improve its classification of brain tumors as well.

In the course of training sessions, the network uses a loss function that measures the difference between the predictions made by the model and the actual values. The goal was to reduce this loss which was a measure of error. Thus, as the network goes through the process for several epochs, it adjusts the weight of neurons in order to minimize the loss function, which in turn enhances classification capability. This learning process helps make the model increasingly accurate in its categorization of the upper bound of possible brain tumors, making it useful for clinical practice.

The optimization process goes on until the network obtains a minimal state where the weights adjustment causes very small improvements over the total network. At this stage the network has mastered the functionality of giving near accurate predictions the functionality that was programmed into it when training the network from MRI images. The obtained model was then used to test its ability to generalize on a different validation set in order to ascertain the ability to classify new MRI images that it has not encountered before. This kind of training where the learning was made alternately and weights are adjusted was crucial for the construction of the deep learning model for the selection of brain tumor.

3 RESULTS AND DISCUSSION

The proposed DCN-PECT framework was experimentally evaluated to analyze its effectiveness in multi-class brain tumor segmentation and classification using PECT/SPECT imaging data. The performance of the proposed model was compared with several existing state-of-the-art approaches including SPGAN-MSOA-CBT, IACO-ResNet, BTSC-TNAS, and PSO-KELM. The evaluation was carried out using multiple quantitative performance metrics such as precision, recall, specificity, G-Mean, accuracy, Dice Score, and execution time. These metrics were selected because they provide comprehensive insight into both classification and segmentation performance, which are essential for reliable medical image analysis.

The experimental evaluation demonstrates that the proposed DCN-PECT framework significantly improves the classification and segmentation capability when compared with conventional and recently developed deep learning approaches. The obtained results validate the effectiveness of the proposed DenseNet-based feature extraction and multi-class segmentation strategy in accurately identifying tumor regions and differentiating them from healthy tissues.

The categorical cross-entropy loss function used during training is mathematically represented as:

$$L = -\frac{1}{N}\sum_{i=1}^{N}\sum_{j=1}^{C} m_{ij} y_{ij} \log(p_{ij}), \tag{1}$$

where y_{ij} denotes the ground truth label, p_{ij} represents the predicted probability, N indicates the total number of samples, and C corresponds to the number of output classes. The loss function minimizes the discrepancy between actual and predicted class labels and assists the network in improving segmentation and classification performance during training.

The Dice Similarity Coefficient (DSC), which evaluates the overlap between predicted segmentation and ground truth segmentation, is given by:

$$DSC = \frac{1}{C}\sum_{j=1}^{C} \frac{2\sum_{i=1}^{N} p_{ij} y_{ij}}{\sum_{i=1}^{N} p_{ij} + \sum_{i=1}^{N} y_{ij}}. \tag{2}$$

The Dice Score is highly important in medical image segmentation because it directly measures tumor boundary accuracy and segmentation quality.

Precision and recall are calculated using:

$$P_j = \frac{TP_j}{TP_j + FP_j}, \tag{3}$$

$$R_j = \frac{TP_j}{TP_j + FN_j}, \tag{4}$$

where TP_j, FP_j, and FN_j denote true positives, false positives, and false negatives, respectively. Precision evaluates the correctness of positive predictions, while recall measures the ability of the model to identify all actual positive samples.

The F1-score and Macro-F1 score are represented as:

$$F1_j = 2 \times \frac{P_j \times R_j}{P_j + R_j}, \tag{5}$$

$$Macro\text{-}F1 = \frac{1}{C}\sum_{j=1}^{C} F1_j. \tag{6}$$

The F1-score provides a balanced measure between precision and recall and is highly useful in evaluating imbalanced medical datasets.

Specificity and G-Mean are mathematically expressed as:

$$S_j = \frac{TN_j}{TN_j + FP_j}, \tag{7}$$

$$G\text{-}Mean = \sqrt{\frac{1}{C}\sum_{j=1}^{C} S_j \times R_j}. \tag{8}$$

Specificity measures the capability of the framework to correctly identify healthy tissues, while G-Mean evaluates the balance between sensitivity and specificity.

The softmax activation function used for multi-class probability estimation is defined as:

$$P_{ij} = \frac{\exp(z_{ij})}{\sum_{k=1}^{C} \exp(z_{ik})}. \tag{9}$$

The Intersection over Union (IoU) metric used for segmentation evaluation is represented as:

$$IoU_j = \frac{\sum_{i=1}^{N} p_{ij} y_{ij}}{\sum_{i=1}^{N} (p_{ij} + y_{ij} - p_{ij} y_{ij})}. \tag{10}$$

The weight update process using gradient descent optimization is represented as:

$$w_{t+1} = w_t - \eta \sum_{j=1}^{C} \frac{\partial L_j}{\partial w_t}, \tag{11}$$

where η denotes the learning rate and w_t represents the network weights during iteration t.

The comparative performance analysis of the proposed DCN-PECT technique and existing approaches is summarized in Table 1. The obtained results clearly indicate that the proposed framework achieved superior performance across all evaluation metrics.

The precision analysis presented in Table 1 demonstrates that the proposed DCN-PECT framework achieved the highest precision value of 92.77 %. Precision

Methods	Prec.	Rec.	Spec.	G-Mean	Acc.	Dice	Time (s)
SPGAN-MSOA-CBT	78.35	90.23	67.81	78.22	75.32	0.852	5.873
IACO-ResNet	87.34	91.11	72.67	81.36	71.56	0.840	4.225
BTSC-TNAS	85.67	92.21	81.88	86.89	86.88	0.837	2.998
PSO-KELM	91.45	93.26	92.87	93.06	82.71	0.841	2.117
Proposed DCN-PECT	**92.77**	**94.11**	**94.16**	**94.13**	**94.29**	**0.855**	**1.163**

Table 1. Comparative analysis for DCN-PECT technique

is highly important in medical diagnosis because it measures the proportion of correctly classified tumor regions among all predicted tumor samples. Higher precision values indicate lower false positive rates and improved diagnostic reliability. Existing methods such as SPGAN-MSOA-CBT and IACO-ResNet produced lower precision values due to limitations in accurately extracting discriminative tumor features from complex PECT/SPECT images. The proposed DCN-PECT framework successfully overcame these limitations by employing DenseNet-based feature learning and multi-class segmentation mechanisms.

Similarly, the recall performance of the proposed framework reached 94.11 %, which was higher than all comparative methods. Recall measures the capability of the framework to identify all actual tumor instances correctly. High recall values are particularly important in clinical diagnosis because missed tumor detection may lead to severe treatment delays and reduced survival rates. The proposed framework achieved superior recall because of its ability to preserve spatial and contextual information during feature extraction and segmentation.

The specificity analysis further confirms the effectiveness of the proposed DCN-PECT framework. The achieved specificity value of 94.16 % demonstrates the capability of the proposed model to accurately distinguish healthy tissue regions from tumor regions. In comparison, SPGAN-MSOA-CBT produced significantly lower specificity due to its limited robustness in handling imaging noise and tissue variability. The proposed framework effectively minimized false positive classifications through optimized segmentation and improved feature representation learning.

The G-Mean metric validates the balanced classification capability of the proposed model. The proposed DCN-PECT achieved the highest G-Mean value of 94.13 %, indicating stable and balanced performance between sensitivity and specificity. This balanced performance is highly important in medical imaging applications because both tumor detection and healthy tissue preservation are clinically significant.

The classification accuracy of the proposed framework reached 94.29 %, which was considerably higher than all comparative methods. The improved accuracy demonstrates the effectiveness of the proposed architecture in handling complex tumor structures and variations in brain tumor characteristics. The DenseNet architecture contributed significantly toward extracting hierarchical feature representations, which improved the segmentation and classification capability of the proposed model.

The Dice Score analysis further confirms the segmentation superiority of the proposed framework. The obtained Dice Score of 0.855 indicates strong overlap between predicted tumor regions and ground truth segmentation masks. Accurate tumor boundary delineation is essential in neuro-oncology applications because treatment planning and prognosis estimation depend significantly on segmentation quality. The proposed framework successfully preserved tumor boundaries and structural details through multi-class segmentation learning.

Execution time analysis also demonstrates the computational efficiency of the proposed framework. The proposed DCN-PECT achieved the minimum execution time of 1.163 s, which was significantly lower than all comparative approaches. Faster execution time is highly desirable in real-time clinical environments where rapid diagnosis and treatment planning are essential. The reduced execution time was achieved through optimized network architecture design and efficient convolutional feature extraction.

The dataset distribution used for experimentation is summarized in Table 2. The dataset consisted of multiple brain tumor categories including glioma, meningioma, and pituitary tumors. The use of a diverse dataset improved the robustness and generalization capability of the proposed framework.

Tumor Type	**Number of Images**
Glioma	1 426
Meningioma	708
Pituitary Tumor	930

Table 2. Distribution of Brain Tumor Dataset

Glioma images constituted the largest portion of the dataset due to their high prevalence and structural complexity. The dataset diversity enabled the proposed framework to learn different tumor patterns and improve classification robustness under varying imaging conditions.

Figure 2 illustrates the training and validation accuracy and loss analysis of the proposed DCN-PECT framework. The training and validation accuracy gradually increased with increasing epochs, indicating effective learning behavior and stable convergence of the network. Simultaneously, the training and validation loss continuously decreased during training, confirming reduction in prediction error and optimization of network parameters. The similarity between training and validation curves indicates that the proposed framework achieved good generalization capability without significant overfitting.

Figure 3 presents the grading analysis of malignant tumors identified by the proposed framework. Accurate tumor grading is essential in clinical diagnosis because treatment planning and prognosis estimation depend strongly on tumor severity.

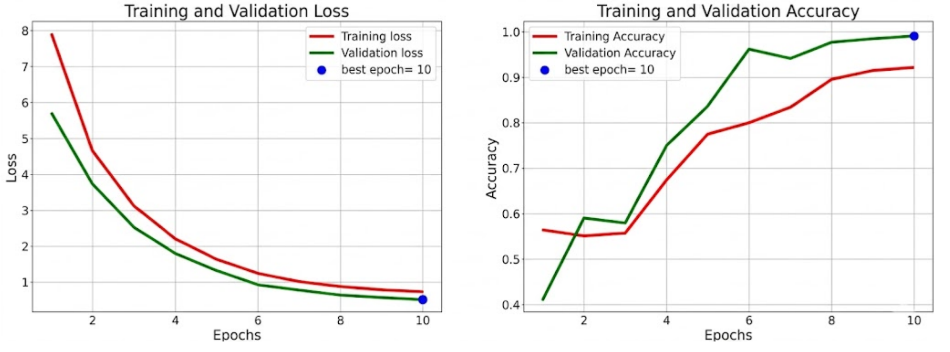

Figure 2. Training and validation loss and accuracy analysis

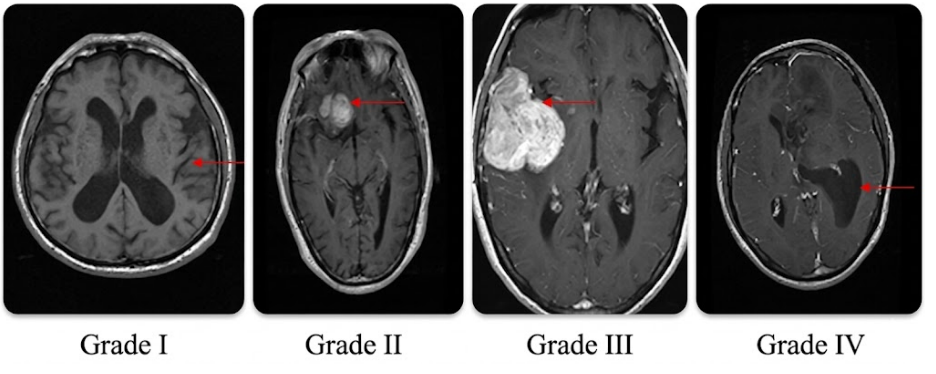

Figure 3. Grade of malignant tumors

The proposed DCN-PECT framework effectively differentiated tumor grades based on pathological characteristics and imaging features.

Sample images from the dataset are illustrated in Figure 4. The dataset contains significant variations in tumor shape, size, intensity, and spatial distribution, which increases the complexity of segmentation and classification tasks. The proposed framework successfully handled these variations through deep convolutional learning and multi-class segmentation strategies.

Overall, the experimental results demonstrate that the proposed DCN-PECT framework significantly outperformed existing state-of-the-art approaches in terms of classification accuracy, segmentation quality, computational efficiency, and robustness. The integration of DenseNet-based deep learning architecture with multi-class segmentation maps enabled effective extraction of discriminative tumor features and improved diagnostic reliability. The obtained results confirm the potential of the proposed framework for practical medical imaging applications and advanced brain tumor diagnosis systems.

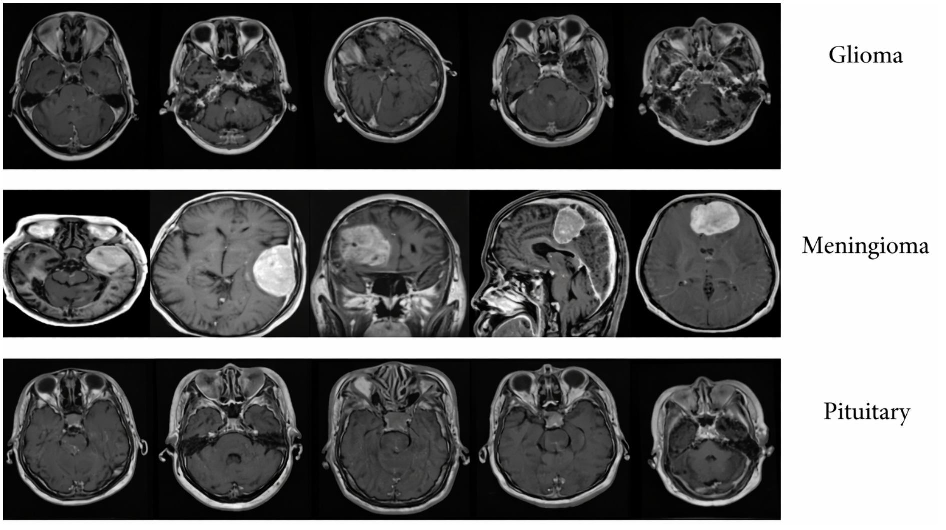

Figure 4. Sample images for dataset

4 CONCLUSION

Iterative improvements in deep learning models and segmentation techniques significantly enhance brain tumor classification performance. Progressive increases in performance demonstrate the effectiveness of advanced methodologies, particularly multi-class segmentation and deep learning models, in improving diagnostic accuracy. Careful model optimization and architectural refinement play a crucial role in achieving meaningful and reliable results in medical imaging. Furthermore, machine learning and artificial intelligence exhibit growing potential in clinical diagnostics, especially for accurate and timely tumor detection and classification. Sophisticated deep learning models, when properly trained and validated, have the capability to outperform conventional diagnostic techniques. The stability observed in high-performing configurations suggests that current methodologies may have reached an optimal performance threshold, with only marginal gains from incremental improvements. Therefore, further transformative innovations are required to achieve significant advancements beyond existing approaches. Nonetheless, current methods can be effectively applied in clinical practice, enabling efficient and accurate brain tumor diagnosis. Continuous advancements in deep learning and segmentation techniques remain essential for the evolution of medical imaging and diagnostic systems. Overall, these technologies hold great promise in contributing to precision medicine by enhancing healthcare quality and advancing diagnostic capabilities.

REFERENCES

[1] Najjar, R.: Redefining Radiology: A Review of Artificial Intelligence Integration in Medical Imaging. Diagnostics, Vol. 13, 2023, No. 17, Art. No. 2760, doi: 10.3390/diagnostics13172760.

[2] Berle, B. F.: 3D Modelling of Brain Metastasis Microenvironment for Evaluation of Tumour-Stromal Interactions. Ph.D. Thesis. University of Bergen, 2023.

[3] Ostrom, Q. T.—Patil, N.—Cioffi, G.—Waite, K.—Kruchko, C.—Barnholtz-Sloan, J. S.: CBTRUS Statistical Report: Primary Brain and Other Central Nervous System Tumors Diagnosed in the United States in 2013–2017. Neuro-Oncology, Vol. 22, 2020, No. Supplement 1, pp. iv1–iv96, doi: 10.1093/neuonc/noaa200.

[4] Li, W.—Liang, H.—Wang, W.—Liu, J.—Liu, X.—Lao, S.—Liang, W.—He, J.: Global Cancer Statistics for Adolescents and Young Adults: Population Based Study. Journal of Hematology & oncology, Vol. 17, 2024, No. 1, Art. No. 99, doi: 10.1186/s13045-024-01623-9.

[5] Choi, J. H.—Ro, J. Y.: The 2020 WHO Classification of Tumors of Soft Tissue: Selected Changes and New Entities. Advances in Anatomic Pathology, Vol. 28, 2021, No. 1, pp. 44–58, doi: 10.1097/PAP.0000000000000284.

[6] Wang, L. M.—Englander, Z. K.—Miller, M. L.—Bruce, J. N.: Malignant Glioma. In: Rezaei, N., Hanaei, S. (Eds.): Human Brain and Spinal Cord Tumors: From Bench to Bedside. Volume 2. Springer, Cham, Advances in Experimental Medicine and Biology, Vol. 1405, 2023, pp. 1–30, doi: 10.1007/978-3-031-23705-8_1.

[7] Seker-Polat, F.—Pinarbasi Degirmenci, N.—Solaroglu, I.—Bagci-Onder, T.: Tumor Cell Infiltration into the Brain in Glioblastoma: From Mechanisms to Clinical Perspectives. Cancers, Vol. 14, 2022, No. 2, Art. No. 443, doi: 10.3390/cancers14020443.

[8] Fernandes, S. L.—Tanik, U. J.—Rajinikanth, V.—Karthik, K. A.: A Reliable Framework for Accurate Brain Image Examination and Treatment Planning Based on Early Diagnosis Support for Clinicians. Neural Computing and Applications, Vol. 32, 2020, No. 20, pp. 15897–15908, doi: 10.1007/s00521-019-04369-5.

[9] Liu, B.—Zhou, H.—Tan, L.—Siu, K. T. H.—Guan, X. Y.: Exploring Treatment Options in Cancer: Tumor Treatment Strategies. Signal Transduction and Targeted Therapy, Vol. 9, 2024, No. 1, Art. No. 175, doi: 10.1038/s41392-024-01766-8.

[10] Adekunle, J. J.—Ike-Okpe, O. I.—Abiodun, W. O.—Lawal, M. M.—Igweh, C. J.: Brain Tumor Detection System: Revolutionizing Diagnosis with Technology. International Journal of Health Research and Physical Study, Vol. 5, 2024, No. 3, pp. 18–35.

[11] Slegers, R. J.—Blumcke, I.: Low-Grade Developmental and Epilepsy Associated Brain Tumors: A Critical Update 2020. Acta Neuropathologica Communications, Vol. 8, 2020, No. 1, Art. No. 27, doi: 10.1186/s40478-020-00904-x.

[12] Bogdańska, M. U.—Bodnar, M.—Piotrowska, M. J.—Murek, M.—Schucht, P.—Beck, J.—Martínez-González, A.—Pérez-García, V. M.: A Mathematical Model Describes the Malignant Transformation of Low

Grade Gliomas: Prognostic Implications. PLoS ONE, Vol. 12, 2017, No. 8, Art. No. e0179999, doi: 10.1371/journal.pone.0179999.

[13] Lalitha, S.—Sanjana, T.—Bhavana, H. T.—Bhan, I.—Harshith, G.: Medical Imaging Modalities and Different Image Processing Techniques: State of the Art Review. In: Shinde, S. V., Mahalle, P. N., Bendre, V., Castillo, O. (Eds.): Disruptive Developments in Biomedical Applications. CRC Press, 2022, pp. 17–36, doi: 10.1201/9781003272694-3.

[14] Swain, S.—Muduli, K.—Kommula, V. P.—Sahoo, K. K.: Innovations in Internet of Medical Things, Artificial Intelligence, and Readiness of the Healthcare Sector Towards Health 4.0 Adoption. International Journal of Social Ecology and Sustainable Development (IJSESD), Vol. 13, 2022, No. 1, pp. 1–14, doi: 10.4018/IJSESD.292078.

[15] Ghorbian, M.—Ghorbian, S.—Ghobaei-Arani, M.: A Comprehensive Review on Machine Learning in Brain Tumor Classification: Taxonomy, Challenges, and Future Trends. Biomedical Signal Processing and Control, Vol. 98, 2024, Art. No. 106774, doi: 10.1016/j.bspc.2024.106774.

[16] Waite, S.—Grigorian, A.—Alexander, R. G.—Macknik, S. L.—Carrasco, M.—Heeger, D. J.—Martinez-Conde, S.: Analysis of Perceptual Expertise in Radiology – Current Knowledge and a New Perspective. Frontiers in Human Neuroscience, Vol. 13, 2019, Art. No. 213, doi: 10.3389/fnhum.2019.00213.

[17] Haleem, A.—Javaid, M.—Singh, R. P.—Suman, R.: Medical 4.0 Technologies for Healthcare: Features, Capabilities, and Applications. Internet of Things and Cyber-Physical Systems, Vol. 2, 2022, pp. 12–30, doi: 10.1016/j.iotcps.2022.04.001.

[18] Ngugi, L. C.—Abelwahab, M.—Abo-Zahhad, M.: Recent Advances in Image Processing Techniques for Automated Leaf Pest and Disease Recognition – A Review. Information Processing in Agriculture, Vol. 8, 2021, No. 1, pp. 27–51, doi: 10.1016/j.inpa.2020.04.004.

[19] Obuchowicz, R.—Strzelecki, M.—Piórkowski, A.: Clinical Applications of Artificial Intelligence in Medical Imaging and Image Processing – A Review. Cancers, Vol. 16, 2024, No. 10, Art. No. 1870, doi: 10.3390/cancers16101870.

[20] Milgrom, B.—Avrahamy, R.—David, T.—Caspi, A.—Golovachev, Y.—Engelberg, S.: Extended Depth-of-Field Imaging Employing Integrated Binary Phase Pupil Mask and Principal Component Analysis Image Fusion. Optics Express, Vol. 28, 2020, No. 16, pp. 23862–23873, doi: 10.1364/OE.393037.

[21] Poldrack, R. A.—Mumford, J. A.—Nichols, T. E.: Handbook of Functional MRI Data Analysis. Cambridge University Press, 2024.

[22] Hussain, S.—Nascimento, M.—Joseph, D.: Nonlinear Demosaicking Method and Apparatus for Nonlinear CMOS Image Sensors Exhibiting Low-Density Salt-and-Pepper Noise. Journal of Electronic Imaging, Vol. 32, 2023, No. 2, Art. No. 023004, doi: 10.1117/1.JEI.32.2.023004.

[23] Algan, G.—Ulusoy, I.: Image Classification with Deep Learning in the Presence of Noisy Labels: A Survey. Knowledge-Based Systems, Vol. 215, 2021, Art. No. 106771, doi: 10.1016/j.knosys.2021.106771.

[24] Singh, R.—Singh, N.—Kaur, L.: Deep Learning Methods for 3D Magnetic Resonance Image Denoising, Bias Field and Motion Artifact Correction: A Comprehensive

Review. Physics in Medicine and Biology, Vol. 69, 2024, No. 23, Art. No. 23TR01, doi: 10.1088/1361-6560/ad94c7.

[25] Jiang, X.—Hu, Z.—Wang, S.—Zhang, Y.: Deep Learning for Medical Image-Based Cancer Diagnosis. Cancers, Vol. 15, 2023, No. 14, Art. No. 3608, doi: 10.3390/cancers15143608.

[26] Ramesh, K. K. D.—Kumar, G. K.—Swapna, K.—Datta, D.—Rajest, S. S.: A Review of Medical Image Segmentation Algorithms. EAI Endorsed Transactions on Pervasive Health and Technology, Vol. 7, 2021, No. 27, Art. No. e6, doi: 10.4108/eai.12-4-2021.169184.

[27] Swain, S.—Oyekola, P. O.—Muduli, K.: Intelligent Technologies for Excellency in Sustainable Operational Performance in the Healthcare Sector. International Journal of Social Ecology and Sustainable Development (IJSESD), Vol. 13, 2022, No. 5, pp. 1–16, doi: 10.4018/IJSESD.313963.

[28] Prabhod, K. J.—Gadhiraju, A.: Foundation Models in Medical Imaging: Revolutionizing Diagnostic Accuracy and Efficiency. Journal of Artificial Intelligence Research and Applications, Vol. 4, 2024, No. 1, pp. 471–511.

[29] Soomro, T. A.—Ali, A.—Jandan, N. A.—Afifi, A. J.—Irfan, M.—Alqhtani, S.—Glowacz, A.—Alqahtani, A.—Tadeusiewicz, R.—Kantoch, E.—Zheng, L.: Impact of Novel Image Preprocessing Techniques on Retinal Vessel Segmentation. Electronics, Vol. 10, 2021, No. 18, Art. No. 2297, doi: 10.3390/electronics10182297.

[30] Abdel-Nabi, H.—Ali, M.—Awajan, A.—Daoud, M.—Alazrai, R.—Suganthan, P. N.—Ali, T.: A Comprehensive Review of the Deep Learning-Based Tumor Analysis Approaches in Histopathological Images: Segmentation, Classification and Multi-Learning Tasks. Cluster Computing, Vol. 26, 2023, No. 5, pp. 3145–3185, doi: 10.1007/s10586-022-03951-2.

[31] Joshi, R. C.—Sharma, A. K.—Dutta, M. K.: VisionDeep-AI: Deep Learning-Based Retinal Blood Vessels Segmentation and Multi-Class Classification Framework. Biomedical Signal Processing and Control, Vol. 94, 2024, Art. No. 106273, doi: 10.1016/j.bspc.2024.106273.

[32] Jiménez, G.—Racoceanu, D.: Computational Pathology for Brain Disorders. In: Colliot, O. (Ed.): Machine Learning for Brain Disorders. Humana, New York, NY, Neuromethods, Vol. 197, 2023, pp. 533–572, doi: 10.1007/978-1-0716-3195-9_18.

[33] Mahmood, T.—Rehman, A.—Saba, T.—Nadeem, L.—Bahaj, S. A. O.: Recent Advancements and Future Prospects in Active Deep Learning for Medical Image Segmentation and Classification. IEEE Access, Vol. 11, 2023, pp. 113623–113652, doi: 10.1109/ACCESS.2023.3313977.

[34] Sony, S.—Dunphy, K.—Sadhu, A.—Capretz, M.: A Systematic Review of Convolutional Neural Network-Based Structural Condition Assessment Techniques. Engineering Structures, Vol. 226, 2021, Art. No. 111347, doi: 10.1016/j.engstruct.2020.111347.

[35] Xu, Y.—Quan, R.—Xu, W.—Huang, Y.—Chen, W.—Liu, F.: Advances in Medical Image Segmentation: A Comprehensive Review of Traditional, Deep Learning and Hybrid Approaches. Bioengineering, Vol. 11, 2024, No. 10, Art. No. 1034, doi:

10.3390/bioengineering11101034.

[36] Ma, J.—Jiang, X.—Fan, A.—Jiang, J.—Yan, J.: Image Matching from Handcrafted to Deep Features: A Survey. International Journal of Computer Vision, Vol. 129, 2021, No. 1, pp. 23–79, doi: 10.1007/s11263-020-01359-2.

[37] Gao, X.—Chen, T.—Zang, Y.—Zhang, W.—Hung Nguyen, Q. V.—Zheng, K.—Yin, H.: Graph Condensation for Inductive Node Representation Learning. 2024 IEEE 40th International Conference on Data Engineering (ICDE), 2024, pp. 3056–3069, doi: 10.1109/ICDE60146.2024.00237.

[38] Mohd, M.—Jan, R.—Shah, M.: Text Document Summarization Using Word Embedding. Expert Systems with Applications, Vol. 143, 2020, Art. No. 112958, doi: 10.1016/j.eswa.2019.112958.

[39] Sathya, R.—Saleena, B.: A Framework for Designing Unsupervised Pothole Detection by Integrating Feature Extraction Using Deep Recurrent Neural Network. Wireless Personal Communications, Vol. 126, 2022, No. 2, pp. 1241–1271, doi: 10.1007/s11277-022-09790-z.

J. Hima Bindu is Assistant Professor in the Department of Information Technology at Mahatma Gandhi Institute of Technology, Telangana, India. She completed her B.Tech. in computer science and information technology from the Sai Spurthi Institute of Technology and M.Tech. in computer science from the JNTUH. She is currently pursuing her Ph.D. at the Vignan's Foundation for Science, Technology and Research, a deemed university in the Guntur district, Andhra Pradesh, India. She is a member of the ISTE professional body and has published more than 15 papers in international journals and conferences. Her research interests include deep learning, machine learning, and information security.

M. Uma Devi completed her Ph.D. in computer science from the University of Hyderabad in 2011, specializing in document forensics. She worked as a Junior Research Fellow (JRF) and Senior Research Fellow (SRF) at the Government Examiner of Questioned Documents under the Ministry of Home Affairs. She has a total of 18 years of experience, including 4 years of research and 14 years of teaching. She is currently working as Associate Professor in the Department of Computer Science and Engineering at the Vignan's Foundation for Science, Technology, and Research. Her research interests include printed document forensics, image processing, soft computing, natural language processing, and machine learning. She has published 15 papers in various journals and international conferences and is an active member of professional bodies such as CSI and IAENG.